TU Delft

Delft University of Technology

Polyhydroxyalkanoate production in a biofilm by mixed culture phototrophic bacteria

Hülsen, Tim; Venturato, Daniel; Chan, Clement; Vandi, Luigi; Laycock, Bronwyn; Pratt, Steven; Stegman, Samuel; van Loosdrecht, Mark; Batstone, Damien J.

DOI
10.1016/j.jclepro.2023.140001

Publication date
2024

Document Version
Final published version

Published in
Journal of Cleaner Production

Citation (APA)
Hülsen, T., Venturato, D., Chan, C., Vandi, L., Laycock, B., Pratt, S., Stegman, S., van Loosdrecht, M., & Batstone, D. J. (2024). Polyhydroxyalkanoate production in a biofilm by mixed culture phototrophic bacteria. *Journal of Cleaner Production*, *434*, Article 140001. https://doi.org/10.1016/j.jclepro.2023.140001

Important note
To cite this publication, please use the final published version (if applicable).
Please check the document version above.

Copyright
Other than for strictly personal use, it is not permitted to download, forward or distribute the text or part of it, without the consent of the author(s) and/or copyright holder(s), unless the work is under an open content license such as Creative Commons.

Takedown policy
Please contact us and provide details if you believe this document breaches copyrights.
We will remove access to the work immediately and investigate your claim.

This work is downloaded from Delft University of Technology.
For technical reasons the number of authors shown on this cover page is limited to a maximum of 10.

Journal of Cleaner Production 434 (2024) 140001

Contents lists available at ScienceDirect

Journal of Cleaner Production

journal homepage: www.elsevier.com/locate/jclepro

Polyhydroxyalkanoate production in a biofilm by mixed culture phototrophic bacteria

Tim Hülsen [a], Daniel Venturato [a,b], Clement Chan [c], Luigi Vandi [c], Bronwyn Laycock [c], Steven Pratt [c], Samuel Stegman [a], Mark van Loosdrecht [d], Damien J. Batstone [a,*]

[a] Australian Centre for Water and Environmental Biotechnology, The University of Queensland, Brisbane, QLD, 4072, Australia
[b] Urban Utilities, Brisbane, QLD, 4006, Australia
[c] School of Chemical Engineering, The University of Queensland, Brisbane, QLD, 4072, Australia
[d] Department of Biotechnology, Delft University of Technology, 2628, BC, Delft, the Netherlands

ARTICLE INFO

Handling Editor: Maria Teresa Moreira

Keywords:
Purple phototrophic bacteria
Polyhydroxyalkanoates
Resource recovery
Biofilm

ABSTRACT

Anoxygenic purple phototrophic bacteria (PPB) were utilised in an 80 L biofilm flat plate photobioreactor to generate polyhydroxyalkanoate (PHA) over 44 cycles, with acetate as feed. Over the cycles, net PHA yield (growth + accumulation) averaged 21% while accumulation yield averaged 55%. Average PHA content was 35 wt% volatile solids (VS), with the majority (>80%) being harvested from the biofilm at 100 gTotal solids (TS) L^{-1}. The PPB microbial population averaged 45% of total population. Detailed cycle studies indicated that PHA content (and yield) peaked at 0.5–1 d into the accumulation stage (peak of 53 wt% VS), suggesting that cycle time optimisation could improve both yield and selection of PHA accumulators. The resulting polymeric material was comprised of poly(3-hydroxybutyrate-*co*-3-hydroxyvalerate) with 95.5 mol% 3-hydroxybutyrate and 4.5 mol % 3-hydroxyvalerate content, but the molecular weight, at >1090 kDa, is unusually high for extracted, microbially produced PHA and a feature of this work.

1. Introduction

Demand for bio-based and biodegradable plastics from renewable resources is experiencing substantial growth. This is due to their high functionality, low environmental impact, legislated requirements to eliminate non-degradable plastics from the environment, and consumer preferences (Kourmentza et al., 2017). This has attracted investment in polyhydroxyalkanoates (PHAs), which are bio-based and biodegradable thermopolymers, projected to be the fastest growing family of biopolymers in terms of market demand throughout 2020 to 2025, according to European Bioplastics and nova-Institut (2020).

PHA is only made commercially via microbial accumulation, where it is an energy and carbon storage polymer (Chen, 2009) and has additional functions as a stress protectant (Obruca et al., 2021). The capability to accumulate PHA exists in a broad range of prokaryotes, and is generally triggered by carbon-rich but nutrient limiting conditions (of one or several nutrients) with excess metabolic energy (Castro-Sowinski et al., 2010). A range of substrates can be utilised, including methane, H_2/CO_2, CO, methanol, volatile fatty acids (VFAs) and sugars, as well as hydrolysed and pre-fermented waste streams containing VFAs or sugars (Fradinho et al., 2021; Strong et al., 2016). The most common production mode is aerobic, with metabolic energy provided by oxidation of the substrate. Commercial production is dominated by aerobic pure culture production on sterilised sugars and organic acids (Chen, 2009). Mixed culture approaches have been applied as an alternative approach and are based on selection of PHA accumulating organisms, utilising their competitive advantage of substrate storage over ordinary heterotrophs (Reis et al., 2003).

PHA can be produced on a pure culture by a natively capable, genetically engineered aerobic organism, which natively accumulates PHA when nutrient is limited (Chen, 2010). Common substrates are simple sugars, though more complex organics may be used (Chen, 2010). However, catabolic energy generation results in oxidation of a substantial fraction of substrate to CO_2 and H_2O, with resulting PHA of 30–40% commonly achieved (Reis et al., 2003) compared with a maximum theoretical yield of 48%. PHA contents of 80 wt% volatile suspended solids (VSS) in wild strains and up to 95 wt% VSS in recombinant strains (Chen, 2009) have been reported. Gaseous substrates

* Corresponding author.Australian Centre for Water and Environmental Biotechnology The University of Queensland St LuciaBrisbane4072Australia
E-mail address: d.batstone@uq.edu.au (D.J. Batstone).

https://doi.org/10.1016/j.jclepro.2023.140001
Received 9 July 2023; Received in revised form 5 October 2023; Accepted 27 November 2023
Available online 1 December 2023
0959-6526/© 2023 The Authors. Published by Elsevier Ltd. This is an open access article under the CC BY license (http://creativecommons.org/licenses/by/4.0/).

(such as methane) achieve lower yields to PHA (on COD), in the order of 12–30% (Liu et al., 2020; Revelles et al., 2016), mainly related to the increased energy requirements to fix C1 compounds and low solubility of candidate gases. Mixed culture PHA production relies on a selection process (generally feast-famine), which has been well documented in the literature (Reis et al., 2003). This results in lower yields, due to the need to select, and generally a lower PHA content (Jiang et al., 2012). Currently, PHA costs approximately 3–4 times fossil polyethylenes, with fundamental limitations being either yield on substrate (which is high-cost for pure culture), or microbial PHA content, in the case of mixed culture (Werker et al., 2014).

A low net yield on substrate under aerobic conditions is due to the need to use a fraction of the substrate to deliver metabolic energy via oxidative catabolism (theoretical limit 0.48 gCOD $gCOD^{-1}$) (Salehizadeh and Van Loosdrecht, 2004). An alternative to delivering metabolic energy through oxidative respiration is to deliver it via infrared light, utilising phototrophic bacteria (specifically purple phototrophic bacteria (PPB)), (Harada et al., 2008). These organisms can accumulate PHA under anaerobic conditions, utilising infrared light to generate metabolic energy and substrate to form biomass (with nutrients), or PHA (without nutrients). This can increase chemical yield towards unity (Capson-Tojo et al., 2020), and the use of infrared light as energy source under anaerobic conditions eliminates competing aerobic heterotrophs (Hülsen et al., 2019).

As such, the use of PPB for PHA production from pure cultures has been historically researched, and their use in mixed cultures is a current research focus (Montiel-Corona and Buitrón, 2021; Sali and Mackey, 2021).

However, the majority of research has been in pure cultures (predominantly *Rhodobacter sphaeroides*), generally grown on acetic acid and in short batch tests, focusing almost exclusively on the accumulation phase, omitting time and COD required for the growth phase (*e.g.* to calculate rates and yields) (Sali and Mackey, 2021). Average PHA contents of 25 wt% TS (n = 35) were achieved (Capson-Tojo et al., 2020), with a calculated yield of 0.4 gCOD $gCOD^{-1}$. Several works employed mixed PPB cultures, focusing on the accumulation stage, with peak contents between 20 and 60 wt% VSS (Fradinho et al., 2021). None of the studies described the molecular characteristics of the produced PHA and studies addressing these, especially in mixed PPB culture, are rare (Higuchi-Takeuchi et al., 2016). Mixed culture PPB-PHA processes are economically interesting, since low value substrates can be used, and there is culture selection through the use of infrared light (Montiel-Corona and Buitrón, 2021). However, in this case, both the requirements of the PHA accumulation and selection steps need to be considered in determining overall yield.

This study employed an attached biofilm photobioreactor (PBR) to accumulate PHA in a concentrated form and compare biofilm and suspended contents. We aimed to determine the peak and sustained PHA contents, productivities, and the biomass as well as the PHA yields (based on COD), overall and separately over the growth and the accumulation phases, utilising a mixed PPB culture on synthetic media in a reactor operated over multiple batch cycles. Importantly, we also assess the as-produced PHA material properties, identifying the potential for PPB for PHA production in comparison with other production platforms.

2. Material and methods

Mixed culture phototrophic PHA production was investigated in an 80 L photobioreactor (PBR), using synthetic medium as feed over 208 d (44 cycles). The system was operated in sequenced batch mode (75% fresh feed, 25% inoculum), with separate growth (nutrient rich) and accumulation (nutrient limited) stages within a given cycle. The system was operated as an attached biofilm system, with both biofilm and flocculent phases being separately analysed.

2.1. Inoculum and feed

Inoculum was grown in a 10 L Schott bottle of synthetic-media enriched PPB from another experiment (Stegman et al., 2021) as per Hülsen et al. (2014) and fed with media containing: 266 mg$MgSO_4 \cdot 7H_2O$, 75 mg$CaCl_2$, 175mg$FeSO_4 \cdot 7H_2O$, 7 mgEDTA, 7 mgyeast extract, 190 mg K_2HPO_4, 125 mg KH_2PO_4 and 1 mL trace element solution (per L). Glacial acetic acid (HAc) and ammonium chloride were used as a carbon (700 mgCOD L^{-1}) and nitrogen source (35 mgN L^{-1}), respectively. The medium was neutralised with 4 M NaOH (reactor pH 6–6.5) prior to the inoculum addition.

2.2. Photobioreactor

The PBR was an acrylic tank (L x H x W: 100 × 100 × 8 cm (total volume 80 L), with 0.015 m wall-thickness), with a detachable lid, fastened via six clamps and held in a HDPE stand. The lid was not gas tight and the headspace was not flushed to maintain anaerobic conditions. The illuminated reactor surface area was 0.6 m^2 per wall (1.2 m^2 per PBR, illuminated area being lost due to the reactor stands and fill level). The PBR was covered with UV-VIS absorbing foil (Lee Filter: ND 1.2 299, Transformation Tubes) and illuminated continuously with six 150 W fluorescent lights (Nelson clamp flood light), from both sides, at 250 W m^{-2} (on the outside of the foil). Around 80% of the light (mainly UV-VIS) was attenuated by the foil and the Perspex wall, resulting in 48 W m^{-2} in the reactor. Reactor liquid was continuously recycled at 25 L min^{-1} with a pump (0.37 kW, CP00251C1R8C, NOV Australia Pty Ltd) to mix the system. DO and temperature (Mettler Toledo EasySense O2 21) were recorded during sampling. In addition, a 30 L drum served as reservoir to re-inoculate the flat plate photobioreactor (FPPBR) with drained reactor liquid (drum was only used when restarting). A schematic drawing of the system is presented in Fig. 1.

2.3. Photobioreactor operation

The reactor was fed batch wise (75% fresh, 25% inoculum) at an average cycle length of 4.0 d (varying 3–5 d, depending on SCOD consumption), generally divided into a growth and accumulation phase. The first 6 cycles (to 21 d) were growth phase only, to accumulate sufficient biomass on the walls (start-up). During start-up, biomass was scraped from the wall at the end of each phase and resuspended. The system was then operated to 208 d over 38 cycles with 4 d average cycle time (2.5 d average growth, and 1.5 d average accumulation (operation) (see Fig. 3). At the start of the cycle (t_0), the growth phase (GRP) was initiated by adding 60 L of synthetic medium, including all nutrients and

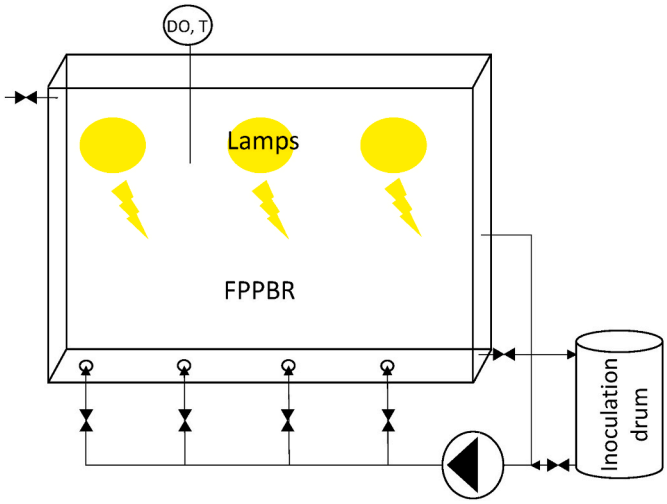

Fig. 1. Flat plate photobioreactor (FPPBR) set-up.

HAc-COD to the 20 L inoculum (collected in the inoculum drum) from the previous cycle. Ammonium was added in concentrations low enough (35 mgN L^{-1}) to be consumed during the 2.5 d during this phase (based on a COD:N ratio of 100:8). The accumulation period (ACC) was initiated with a spike of additional HAc-COD (400 mgCOD L^{-1}). The combined COD addition resulted in a load of around 66 gCOD per batch or 0.27 gCOD L d^{-1}. The pH decrease accompanying the acid addition was adjusted with 1 M NaOH (to 6.0–6.5). The accumulation cycle was finalised (t_f) once the SCOD was consumed. Liquid samples were collected daily to follow the cycles and analysed for pH, total and soluble chemical oxygen demand (TCOD, SCOD), NH_4–N, PO_4–P and volatile fatty acids (VFAs). Temperature and DO were assessed at sampling times. Initial (t_0) and final (t_f) samples were analysed for Total Kjeldahl Nitrogen (TKN) and total phosphorous (TP).

At t_f, the reactor contents were drained slowly (~1.25 L min^{-1}) to prevent resuspension of attached PPB biofilm and 20 L was collected in the inoculation drum (Fig. 1). The effluent was sampled and centrifuged (3270×*g*, 10 min (Allegra™ X-12)), and the centrifuge pellet analysed for PHA content. The biofilm was removed from the wall manually using a squeegee and collected for weighing and mass balance and areal productivity analysis. Biofilm samples were analysed (total and volatile solids (TS, VS), TKN, TP, PHA content and TCOD) while microbial composition (16*S* amplicon sequencing) for both biomass fractions was determined for selected cycles.

2.4. Mass balance closure

Due to the manual harvesting and residual sludge accumulation at the bottom of the reactor after draining, mass balance gaps were unavoidable for individual cycles. To validate that the mass balances closed the following procedure was executed for cycles 33 and 36 (between 133 and 151 d). After draining the reactor, the reactor walls and the bottom were cleaned with tap water. The system was started (t_0) and COD samples were taken ($gCOD_{in}$). At t_{final}, the liquid was drained in three steps, collecting 1/3 of the reactor content (bottom, middle, top). The COD was determined for each fraction (COD samples 1–3). The biofilm was harvested (sample 4). A known amount of water was used to clean the squeegee and the gloves (sample 5). The walls were cleaned with a known amount of water and PPB biomass was collected with the residual biomass at the bottom of the reactor (sample 6). The combined COD samples 1–6, represented the COD_{final}.

2.5. Cycle tests

Over the course of the experiment, two cycle tests were performed (Cycles 20 and 44). Samples were taken at 6 h intervals for 3.75 days. For suspended biomass PHA measurements, 3–10 L of reactor liquid was drained from the reactor and centrifuged. The solids were subsampled for PHA analysis. The remaining solids and the supernatant were mixed and returned to the reactor. This was done carefully to minimise biofilm disturbance. Once a biofilm was sufficiently developed (~1.5 d), biofilm samples were taken after liquid sampling (and draining), to analyse the PHA content. Consecutive biofilm samples were taken from the same area. Liquid samples were also analysed for COD, NH_4–N, VFA and pH.

2.6. Analytical methods

Reactor temperature and dissolved oxygen were monitored by an easySense probe and M200 transmitter (Mettler Toledo). Sample pH was measured using a SevenExcellence™ system (Mettler Toledo). TCOD and SCOD were determined by COD cell tests (Merck, liquid samples: 1.14541.0001, biomass samples: 1.14555.0001). Soluble NH_4–N, NO_2–N, NO_X-N and PO_4–P were determined by Flow Injection Analyzer (FIA) (QuikChem 8500, Lachat Instruments). For cycle studies, NH_4–N test kits (Merck, 1.14752.0001) were used as a real-time ammonium indicator. TKN and TP samples were determined using sulfuric acid, potassium sulfate and copper sulfate catalyst in a block digester (Lachat BD-46, Hach Company, Loveland, CO, USA). VFAs were measured by gas chromatography equipped with a flame ionisation detector (GC-FID) (7890A, Agilent Technologies). All soluble samples were filtered using a 0.45 μm membrane syringe filter (Millex®-HP, Millipore). Total solids were determined by drying at 105 °C for 24 h. Volatile Solids were then determined after 2 h at 550 °C. For PHA contents and for identification of the molar proportions of the 3-hydroxybutyrate (3-HB) and 3-hydroxyvalerate (3-HV) monomer units in the poly(3-hydroxybutyrate-*co*-3-hydroxyvalerate) (PHBV) copolymer, frozen samples (suspended and biofilm) were lyophilised by freeze drying (FD-1-54DD, Kinetics Thermal Systems), digested (20 h at 100 °C) (Ratek Block Dry Digester) in 3% sulfuric acid in methanol and chloroform (Braunegg et al., 1978) (with 200 mg L^{-1} sodium benzoate) solution and analysed by GC-FID (Oehmen et al., 2005).

2.7. Polyhydroxyalkanoate extraction and characterisation

PHA was extracted from the biomass using chloroform as a solvent. 1 g of biomass and 50 mL of chloroform were added into a 100 mL Parr reactor. Note, extraction results in slightly lower measured PHA content compared to direct measurements *e.g.* with thermo-gravimetric analysis (TGA). The reactor was heated to 140 °C and extracted for 2 h under agitation. The solution was filtered through a 0.22 μm PTFE membrane filter using a vacuum filtration apparatus. The filtrate (dissolved PHA in chloroform) was poured into a Petri dish and let evaporate. To remove the carotenoids from the extracted PHA, 100 mL of acetone/methanol (7/2 v/v) was added to the as-extracted PHA and sonicated for 30 min. The solution was filtered using the same procedure as described and the filter cake was dried in a vacuum oven at 60 °C to obtain clean PHA for further characterisation. The quality of the as-extracted PHA, specifically PHBV, in terms of co-monomer composition, molecular weight, thermal properties and thermal stability was compared with commercial PHBV (1.0 mol% 3-hydoxyvalerate (3-HV), TianAn Biologic Materials Co., Ningbo City, China). Extracted PHA weight percentages are expressed on a VS basis.

2.7.1. ^{1}H-nuclear magnetic resonance spectroscopy (^{1}H-NMR)

^{1}H-NMR spectra of the extracted, purified PHBV were recorded using a Bruker Avance 500 MHz high-resolution NMR spectrometer for the determination of the copolymer content. PHA was dissolved in deuterochloroform ($CDCl_3$) (10 mg mL^{-1}). ^{1}H 1D NMR spectra acquisition at 298 K was preceded by 4 dummy scans followed by 64 scans over a spectral width of 11 ppm (5500 Hz). The chemical shifts and the relative peak intensities were determined using the TopSpin 3.5 software. Chemical shifts were referenced to the proton peak of $CDCl_3$ at 7.26 ppm.

2.7.2. Gel permeation chromatography (GPC)

GPC was used to determine the molecular weight of the extracted PHA. PHA samples were dissolved in HPLC grade chloroform (Lichrosolv®, Merck) at 70 °C for 30 min at a concentration of 2.5 mg mL^{-1} in capped glass tubes in a dry block heater (Thermoline Scientific, Model TDB-3). GPC analysis was run using an Agilent 1260 Infinity Multi Detector Suite system (Cheshire, UK). The column set consists of a guard column (Agilent PLgel Guard (5 μm, 7.5 mm × 50 mm)) followed by a series of columns in series: Agilent PLgel 10^5 Å (5 μm, 7.5 mm × 300 mm), Agilent PLgel 10^3 Å (5 μm, 7.5 mm × 300 mm) and Agilent PLgel 100 Å (5 μm, 7.5 mm × 300 mm). The columns were kept at 30 °C. A refractometer and a viscometer, both at 30 °C, were equipped to detect the eluted sample. A chloroform flow rate of 1 mL min^{-1} was used for the analysis. Narrowly distributed molecular weight polystyrene standards were used for calibration and the Mark-Houwink equation was used for molecular weight calculations. The Mark-Houwink constant for polystyrene ($K = 7.2 \times 10^{-5}$ dL g^{-1} and $\alpha = 0.76$) and for P(3HB) in

chloroform (K = 7.7×10^{-5} dL g^{-1} and α = 0.82) were taken from literature.

2.7.3. Differential scanning calorimetry (DSC)

A differential scanning calorimeter Q2000 (TA Instruments) under a constant nitrogen flow of 50 mL min^{-1} was used for thermal (DSC) analysis. The samples were first dried in the vacuum oven at 60 °C for 24 h to remove any absorbed moisture. Samples of 2.0–4.0 mg were placed in a sealed aluminium pan and were analysed using standard DSC heating and cooling scans. Each sample was heated from 25 °C to 185 °C at 10 °C min^{-1} and kept isothermal for 0.1 min, and then cooled to −70 °C at 10 °C min^{-1} and kept isothermal for 5 min. After this, the sample was once again heated to 185 °C at 10 °C min^{-1}. The melting temperature, T_m, and enthalpy of fusion, ΔH_f, of the polymer powder were determined from the 1st heating scan. The melt crystallisation temperature, T_{mc}, was determined from the cooling scan. The glass transition temperature, T_g, was determined from the final heating cycle.

2.7.4. Thermo-gravimetric analysis (TGA)

A Mettler Toledo TGA LF1600 (Mettler Toledo, Switzerland) was used to evaluate the thermal stability of the polymers. Approximately 2 mg of materials were placed in standard 40 μL aluminium crucibles with a pierced aluminium lid, and heated at a rate of 10 °C min^{-1} from 30 °C to 450 °C in air. The air environment was chosen to replicate the conditions found during the extrusion process.

2.8. Microbial community analysis

The microbial community composition of the attached biofilm and the suspended biomass was determined by amplicon sequencing. DNA extraction and subsequent sequencing by Illumina Miseq Platform, using universal primer pair 926F (50-AAACTYAAAKGAATTGACGG-30) and 1392wR (50-ACGGGCGGTGWGTRC-30) primer sets and data analysis was as previously described (Hülsen et al., 2019).

Fluorescence in situ hybridization (FISH) was done with the probes ALF1B (CGTTCGYTCTGAGCCAG) (Manz et al., 1992) for Alpha and some Deltaproteobacteria (red colour) and GAM42a probe (GCCTTCCCACTTCGTTT) for Gammaproteobacteria (green colour). Sample preparation and imaging were described elsewhere (Stegman et al., 2021).

2.9. Data processing and statistical analysis

Inputs are represented as averages and variability in inputs expressed as standard deviation in time-series measurements, represented as $\overline{X}(s_{X_i})$, where $\overline{X}$ is the average value for the data X_i, and s_{X_i} is the standard deviation for the data. Outputs and calculated parameters (including slopes from linear models) are represented as average value, with uncertainty expressed as uncertainty in mean based on a two-tailed *t*-text (95% confidence, 5% significance threshold), represented as $\overline{X} \pm E_{\overline{X}}$, where $E_{\overline{X}}$ is the 95% confidence interval.

3. Results and discussion

3.1. Mass balance and biofilm

The reactor for accumulating PPB was operated for 208 d. PPB attached to the inner submerged, IR irradiated surfaces of the FPPBR. This was indicated by a purple colour biofilm, indicative of carotenoid containing PPB. This biofilm could be recovered between cycles by manual wiping (Fig. 2).

Full operational data for the reactor operation is provided in supplementary information. Cycle time averaged 4 d, and generally ranged from 3 to 5 d (due to manual operation). Uptake of soluble COD was effective, and relatively complete, at a rate of 253 ± 28 mgCOD L^{-1} d^{-1} during growth and 280 ± 36 mg L^{-1} d^{-1} during accumulation (averages across 43 cycles). There was therefore no significant difference in soluble COD uptake rates for growth vs accumulation stages. The residual soluble COD at the end of the growth cycle was 20–100 mgCOD L^{-1}, but organic acid concentrations at the end of growth were always <10 mgCOD L^{-1}. Ammonia was completely taken up during growth. Biofilm coverage averaged 27 gTS m^{-2}, recovered at a wet concentration of 9.7%, >600 times more concentrated compared to the average suspended biomass concentration of 0.15 (0.06) gTS L^{-1}. Biofilm and suspended areal productivities, considering the entire batch, averaged 6.8 ± 0.7 and 2.3 ± 0.3 gTS m^{-2} d^{-1}. The VS contents of both biofilm and suspended biomass were 80–85% (20–15% ash contents).

Evaluating the COD balance across all cycles, 40 ± 4 gCOD was consumed during growth, and 25 ± 3 gCOD was consumed during accumulation for a net consumption of 66 ± 5 gCOD per cycle. Across the 44 growth/accumulation cycles, 49 ± 5 gCOD was recovered from the biofilm, and 14 ± 2 gCOD was recovered from suspension, resulting in 63 ± 6 gCOD per cycle (95% recovery). Detailed balances for cycles 33 and 36 showed 107% and 102%, respectively, of the soluble COD fed was recovered as biomass, with 72% and 80% of the soluble COD fed recovered as biofilm. These data exclude aerobic COD consumption.

3.2. Polyhydroxyalkanoate content and yield

During start-up (Phase 1) the PHA content was low (<13%). Once the accumulation stage was introduced, PHA accumulated fairly consistently with an average of 35 wt% VS at the harvest point at end of cycle (Fig. 3). There was no significant difference between biofilm and suspended biomass PHA content, though the net quantity of PHA in the biofilm was much larger (80% of total PHA in biofilm). The PHA comprised 90% 3-HB and 10% 3-HV monomer units. 3-HV monomers were produced despite no odd chain VFAs (propionate, valerate) being fed or detected at >1 mg L^{-1} during routine analysis. This was also observed by Higuchi-Takeuchi et al. (2016). The 3-HV monomer unit is

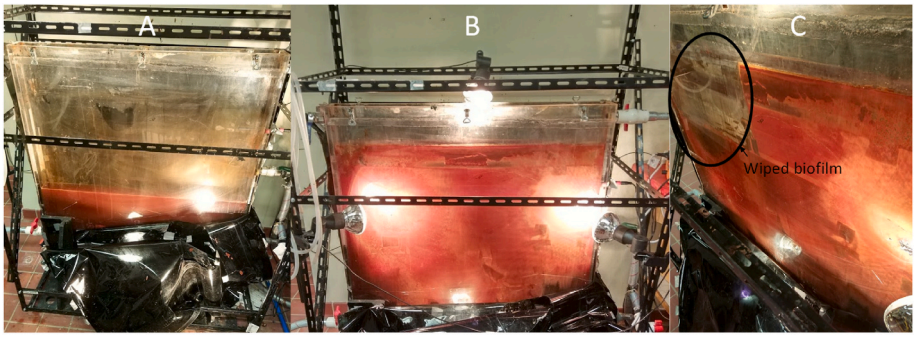

Fig. 2. Representative cycle start with PPB inoculum and cleaned reactor(A), cycle end with biofilm (formed in one cycle) on the inner walls (B) and drained reactor with biofilm (C).

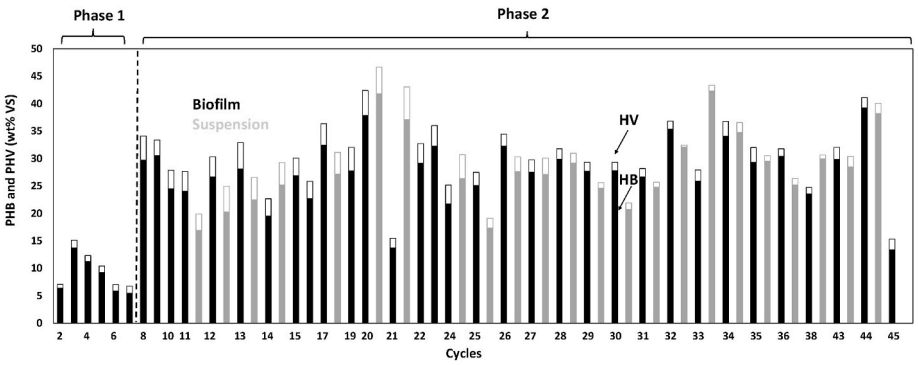

Fig. 3. Weight percentage (based on VS) of 3-HB (solid) and 3-HV (open) monomer units in the biofilm (black) and suspension (grey).

generally formed from odd-chained VFAs. This may be due to a TCA shunt via succinate to propionate, which yields two electrons from acetate, necessary to reduce acetate to PHB (Martínez-Reyes and Chandel, 2020).

PHA recovery per cycle averaged 11 ± 1 gCOD in the biofilm and 2.4 ± 0.7 gCOD in suspension for a total of 13 ± 1 gCOD. This translates to average sustained volumetric and areal productivities of 58 mgPHA-COD L^{-1} d^{-1} and 3.5 gPHA-COD m^{-2} d^{-1}, respectively. The sustained net PHA-COD yield considering all COD fed was 21 ± 3%, or considering VFA fed during accumulation only, was 54 ± 2%. Losses might have incurred due to a combination of biomass growth, alternative carbon storage products, and H_2 production (which was not measured due to the open headspace). The net yield is highly important, especially when growth and accumulation are on the same value substrate, and the growth substrate requirements should not be omitted. This is less relevant when growth takes place with an abundant low-value substrate.

The individual yields per cycle are shown in Fig. 4, and indicate yields per cycle were up to 30% (GRO + ACC + accumulation) in cycle 21, and yield on accumulation only was up to 90%.

3.3. Microbial community

Microbial community data is shown in Fig. 5, and indicates a substantial, but not dominant PPB clade in the community across both biofilm and suspended material. On average, 38 ± 9.9% and 45 ± 12.2% of the community in the suspension and biofilm, respectively, were PPB. The PPB fraction in the biofilm and the suspension were not significantly different ($p = 0.135$). The PPB community was originally a mix of *Rhodopseudomonas* sp., and *Blastochloris* sp. (and traces of *Rubrivivax* sp., *Rhodobacter* sp. and *Rhodoplanes* sp.), but after cycle 13, the relative abundance of *Rhodopseudomonas* sp. decreased while *Allochromatium* sp. emerged, leading to a purple sulfur bacteria dominated system. All major clades *Rhodopseudomonas*, *Allochromatium,* and *Blastochloris* are photoheterotrophs and have been identified to have metabolic or functional capability for PHA accumulation (Fradinho et al., 2021) and to a lesser extent *Blastochloris* sp., which is not extensively covered in the PHA literature. This indicates effective selection for photoheterotrophic PPB.

As reported by Alloul et al. (2019), sludge retention time (SRT) is a driver for PPB microbial community composition, with SRT of less than 0.5 d favouring *Rhodobacter,* and over 0.5 d favouring *Rhodopseudomonas.* Our results reflect this, with *Rhodopseudomonas* initially dominating at an SRT of approximately 4 d (batch) (*Rhodobacter* only present in traces). However, as operation proceeded, *Blastochloris* sp. remained, and *Allochromatium* sp. increased its relative fraction. The emergence of *Allochromatium* may be related to PHA accumulation capability, in which case, further selection could be done by including a famine stage (i.e., light with no substrate). FISH analysis of cycles (t_{final}) 12, 20, 22 and 44 confirmed the results (Supplementary data) where the Alphaproteobacteria abundance also appears to be higher than the relative abundance data. A famine stage would also introduce the possibility to use low value, high nitrogen feeds (such as wastewater) to drive growth and selection, followed by a higher value, low nitrogen feed (*e.g.*, acetate, ethanol or VFA from organic rich wastes) to drive

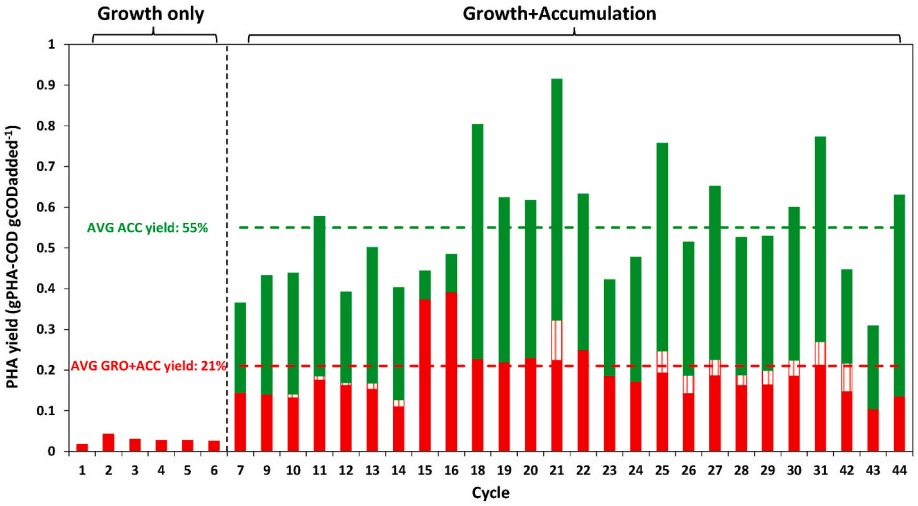

Fig. 4. PHA yields for each complete cycle (GRO + ACC) based on the combined COD added during growth and accumulation phases (GRO + ACC) and yields based on COD dosed during the accumulation phase (ACC) only (green). Overall yield is split between biofilm (deep red), and flocculent (striped red). (For interpretation of the references to colour in this figure legend, the reader is referred to the Web version of this article.)

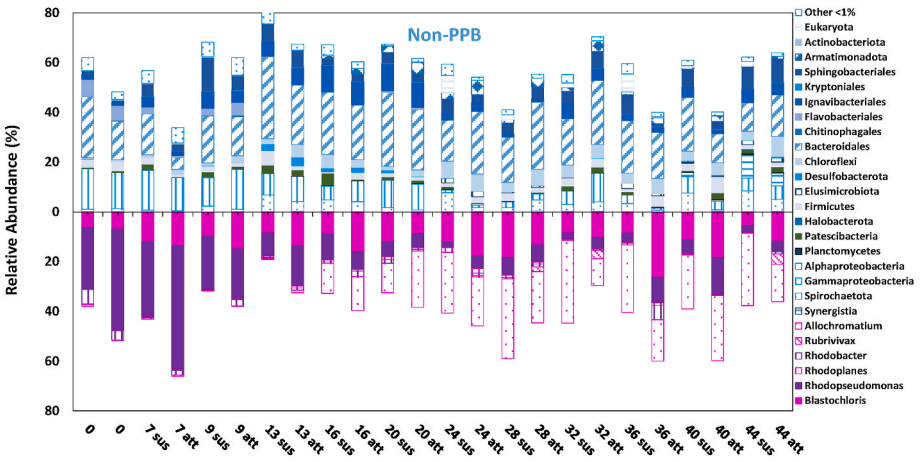

Fig. 5. Microbial community sampled in suspended and attached biomass. "Other PPB" comprises *Rhodocyclaceae*, *Rhodobacter*, and *Rhodoplanes*.

accumulation only. Nitrogen is not the only nutrient which can be limited, and other substrates (*e.g.*, P, Mg, S) could be limited to drive accumulation (Melnicki et al., 2009), which might enable the use of a fermentation broth (from wastewater) as accumulation phase substrate, after precipitation of *e.g.* phosphate and magnesium.

The flanking community was dominated by a diverse range of Bacteriodota (mainly anaerobic Bacteroidales), Firmicutes, Chloroflexi, and other Gammaproteobacteria. The top flanking clades as noted above have been widely identified as flanking or functional elements in aerobic and methylotrophic PHA accumulating systems (Farghaly et al., 2017; Luangthongkam et al., 2019). The role of the non-PPB flanking community needs further investigation, including its actual fraction, functional role, and substrate source (*e.g.*, decay products vs predation). It is not known whether they are functionally accumulating PHA (utilising ATP from proteolytic catabolism), or utilising PHA accumulated by the PPB clades, and this is an important question for system implementation. However, under anaerobic conditions, these organisms cannot grow on acetate only, and we exclude a major role of these bacteria in the PHA accumulation. We further exclude major impacts of O_2 diffusion via the open headspace and subsequent aerobic COD consumption, because of the mass balance closures as described in section 3.1.

It remains a mystery that the relative abundance of PPB is low, at times ~20%, while acetic acid can only be consumed by PPB, methanogens or aerobically with O_2. We also note that the flanking community may be smaller by mass as suggested by the relative abundances (*e.g.*, due to different mean 16S gene copies (Bacteroidales 4.5 *vs. Allochromatium* sp. of 3.0 (Database University of Michigan)). The flanking community may be wholly detrimental, in that they act as a proteolytic agent, removing microbes and PHA, and diluting effective PHA content neutral (essentially only utilising metabolic byproduct), or potentially positive (symbiotically providing growth cofactors). If only 45% of the community is capable of accumulating PHA levels, and the community can be enriched for PPB, the sustained PHA content theoretically increases 2.2 fold to around 78% PHA, assuming a relative PPB abundance of close to 100% (compared with contents observed in *Rhodobacter Sphaeroides* of 82% by Luongo et al. (2017)). In this case, the objective should be to minimise the flanking community, potentially by famine operation as noted above. If the flanking community is anaerobically accumulating PHA, they may have some (potentially synergistic) function in an eventual phototrophic PHA system.

3.4. Cycle studies

Cycle studies for cycles 20 and 44 are shown in Fig. 6(A and B). These show peak PHA contents of 53.2 wt% VS in Cycle 20 compared to 35.9 wt% VS in Cycle 44. SCOD and TCOD removal from liquor were

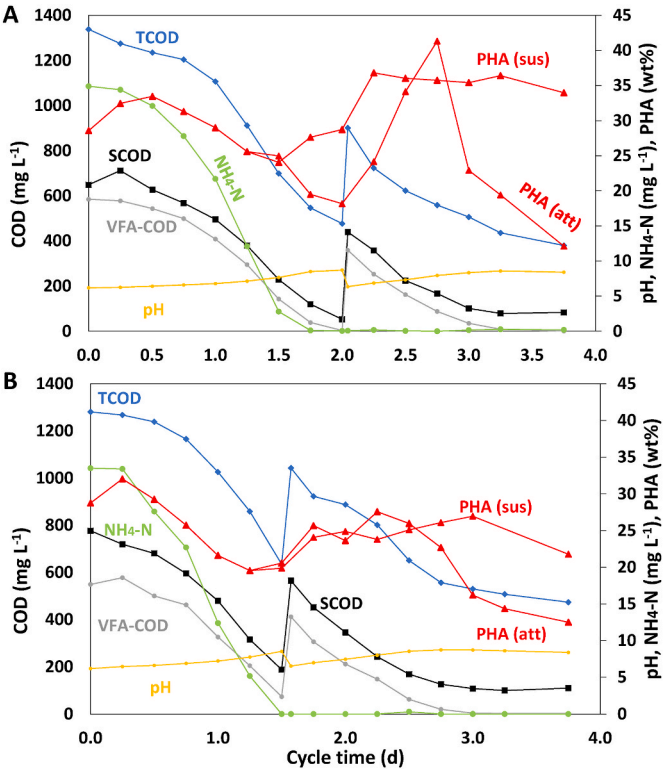

Fig. 6. Ammonium (●), TCOD (◆), SCOD (■), VFA-COD (●), pH (●), PHA of the attached (▲, solid line) and the suspended biomass (▲, hatched line) for Cycles 20 (**A**) and 44 (**B**).

generally correlated, indicating mainly biofilm growth. SCOD uptake rate accelerated during the first 0.5 d, indicating biomass limited conversion, and was then stable at 410 ± 60 mgCOD L^{-1} d^{-1} for cycle 20, and 440 ± 40 mgCOD L^{-1} d^{-1} for cycle 44. Uptake during accumulation was lower (not statistically significant) at 310 ± 100 mgCOD L^{-1} d^{-1} for the first cycle, and 330 ± 60 mgCOD L^{-1} d^{-1} for the second cycle. The SCOD:N uptake ratio of 100:8 indicates that biomass formation dominated during growth (Hülsen et al., 2014).

Both cycles had a peak PHA content, particularly in the biofilm, at 2.5–2.7 d, which indicates that stopping accumulation at this peak point would be important to both maximise PHA yield and enable subsequent extraction. This may also assist in stabilising the community towards PHA accumulators (since they are selected at the peak PHA level for re-

inoculation). Based on the peak production, volumetric PHA productivities were 0.16 gPHA-COD L^{-1} d^{-1} over the entire cycle (COD dosed during GRO + ACC) or 0.62 gPHA-COD L^{-1} d^{-1} over the accumulation phase (COD dosed at the beginning of ACC). This results in a PHA yield of 0.43 gPHA-COD $gHAc\text{-}COD^{-1}_{added}$, over the entire cycle, and 1.1 gPHA-COD $gHAc\text{-}COD^{-1}_{added}$ based on HAc-COD dosed during the accumulation phase. Following this peak, there was a fairly rapid decline, not associated with release of COD to the liquid, indicating this was either transferred to another storage compound, or used for biomass growth (potentially by the flanking community following decay). This behaviour was not seen in suspended biomass to the same extent, where the PHA contents peaked and remained relatively constant afterwards. This may be caused by hydrolysis and availability of nutrients in the dense biofilm, which provides nutrients to grow on the stored PHA as well as potentially N-fixation. PPB are capable of N-fixation. The energy requirement of 1.14 mol_{ATP} gN^{-1} (Hubbell and Kidder, 2009) is compatible with the energy needed to synthesise (or consume) PHA using the common rule of 10 g biomass mol^{-1}_{ATP}. It is quite possible that the biofilm (with sufficient light supply) fixed N_2 into NH_4–N, while biofilm induced shading limited the N fixation in the bulk liquid, and further improvements in yield may be achieved if N_2 can be excluded from the system.

3.5. Extracted polyhydroxyalkanoate properties

3.5.1. Polymer properties – molecular weight and co-monomer content

PHA composition was determined by ^{1}H-NMR and GC analysis. The ^{1}H-NMR spectra are shown in supplementary materials with the peaks corresponding to 3-HB and 3-HV units labelled. The extracted material (collected over the operation period) was found to be 95.5% 3-HB and 4.5 mol% 3-HV PHA. The weight average and number average molecular weights ($\overline{M}_w$ and $\overline{M}_n$) of the material were 1090 and 453 kDa, respectively, which is substantially higher than for commercial PHA *e.g.* 590 and 230 kDa in ENMAT Y1000 (by TianAn Biopolymer, China) (noting that other commercial products have other characteristics). Furthermore, the polydispersity (Đ) of 2.4 (Table 1) was reasonably low for PHA, indicating a relatively narrow molecular weight distribution. In short, the molecular weight of the as-produced PHA is commercially-relevant. The relatively higher $\overline{M}_w$ (and lower Đ) allow for PHA with improved mechanical properties, such as higher impact resistance and toughness, mechanical and tensile strength, and transition temperature (Gentekos et al., 2019) which could amplify its applicability.

3.5.2. Thermal properties

Thermal properties of the synthesised PHA were determined by DSC, with the DSC thermograms being shown in the supplementary materials. Their corresponding thermal properties are summarised in Table 1. The T_m, T_{mc} and T_g were 169 °C, 114 °C and 3.0 °C respectively. All were consistent with literature for 3-HB rich material (Feng et al., 2002). Due to the higher 3-HV content in the extracted PPB PHA, the peak melting temperature decreased with an increase in 3-HV co-monomer content as expected, due to the disturbance of the 3-HB crystalline lattice resulting from the bulkier 3-HV units. The extracted PHA had a lower enthalpy of melting (ΔH_m) than the commercial PHA (Supplementary materials), again as expected. It is important to note here that determining the approximate crystallinity of a PHBV copolymer from the melt enthalpy is not straightforward, since it needs to be calculated relative to the enthalpy of melt of a theoretically 100% crystalline copolymer of the same composition. Pearce and Marchessault (1994), for example, used a reference ΔH_m 100% for 95 mol% 3-HV of 128 J g^{-1}, while Cheng et al. (2009) took their ΔH_m 100% as 146 × mol fraction HB J g^{-1}, since at low 3-HV contents (<10%) the sequences of 3-HV units are excluded from the lamella. Either way, the bulk crystallinity is not much different for the PPB derived PHA compared to the commercial product. A higher melt crystallisation temperature was observed for the PPB derived PHBV (Supplementary materials), indicating that crystallisation of the extracted PHBV was occurring with a lower under-cooling energy (driving force) when compared to the commercial PHBV (Kai et al., 2005). The crystallisation rate can also be estimated by the difference between the starting and ending temperatures (ΔT_c) of the crystallisation peak. The results further indicate that the PPB PHBV had a higher rate of crystallisation than that of the commercial PHBV (with lower 3-HV content) as indicated by a shorter time needed for the completion of crystallisation. Such an observation could be due to the presence of impurities that acted as nucleating agents but further research is required to fully understand the crystal growth behaviour. Close inspection of the heating scan after quench revealed that the T_g of the as-extracted PHA is slightly lower than that of commercial PHA (Supplementary materials). The disparity could be explained by the higher 3-HV content of the extracted PHA. The T_g values of PHBV copolymers decrease with increasing 3-HV content as the distance between molecules is farther given that 3-HV units have a longer side chain (Feng et al., 2002). The segmental mobilities of the copolymer chains are thus lower, resulting in a lower T_g. Overall, the observed differences were consistent with the disparity of composition between the two PHBVs.

3.5.3. Thermal stability

The same conclusions also applied to the thermal stability. The onset of thermal decomposition ($T_{d,\ onset}$) was defined as the temperature at which the specimen weight drops below 95% from the baseline and the peak temperature ($T_{d,\ peak}$) was defined as the temperature at the peak of the derivative curve. Commercial PHA showed better thermal stability than the extracted PPB PHA, with a higher $T_{d,\ peak}$ value (Supplementary materials). The commercial PHA was produced using pure culture biotechnology with sterilisation requirements. On the other hand, the PPB accumulation was performed using mixed culture under non-sterile conditions. The disparity in thermal stability could be due to the presence of small amounts of residual cations or impurities, such as carotenoids, from the accumulation process in the as-extracted polymer or to trace metal impurities, which are known to promote PHA degradation during processing (Werker et al., 2010). The supplementary materials showed the ^{1}H-NMR spectra of the as-extracted PHA before and after carotenoids extraction. A collection of unidentified peaks was observed from the pre-extraction spectra corresponding the complex structure of carotenoid mixture. Those peaks were significantly reduced after the acetone/methanol extraction although still seen at very low

Table 1
Molecular and thermal properties of commerical and as-extracted PHBV.

Sample	Molecular characteristics			Melting behaviour				Crystallisation behaviour				Re-melting behaviour			
	$\overline{M}_n$	$\overline{M}_w$	Đ	*Peak* T_m	*Start* T_m	*End* T_m	ΔH_m	T_{mc}	*Start* T_m	*End* T_m	ΔH_c	*Peak* T_m	*Start* T_m	*End* T_m	ΔH_m
	(kDa)	*(kDa)*	*(–)*	(°C)	(°C)	(°C)	(J g^{-1})	(°C)	(°C)	(°C)	(J g^{-1})	(°C)	(°C)	(°C)	(J g^{-1})
Commercial PHBV (1.0 mol % 3-HV)	198 ± 8	640 ± 40	3.2 ± 0.1	171	138	180	97.8	108	124	70	91.7	170	120	177	97.8
As-extracted PHBV from this study (4.5 mol% 3-HV)	453 ± 7	1090 ± 130	2.4 ± 0.3	148/ 169	107	178	77.3	114	127	77	79	168	114	178	86.3

concentration. We note, non-optimised conventional extraction method (chloroform extraction followed by acetone/methanol cleaning) was used. Literature has shown that the adverse effect can be mitigated by optimising and tailoring the extraction steps to this reported system (Chan et al., 2017), which is the clear next step to improve the processability of the prototype mixed culture PHBV. For the industrial applications, green solvents might be applied (*e.g.* eutectic solvents) combined with peroxide and acids.

Overall, the properties of the generated PHA are promising and consistent with commercially available high 3-HB PHA, (*e.g.* Tianan PHA (1% 3-HV)). The inclusion of 3-HV only becomes important at contents >20% 3-HV, which might be achieved with odd numbered VFAs, *e.g.* to increase the elasticity of the biodegradable material.

While PPB are known to generate high molecular weight PHA, the M_w recorded here are quite significant. This material could potentially be used to make thin films, which generally requires $M_w > 10^6$ Da to blow. This also protects against thermal degradation and related property loss. In conjunction with relatively low polydispersity (lower than published for other PPBs but in line with biomass derived PHA) the high Mw indicates the potential for excellent mechanical properties.

3.6. Performance and industrial significance for PHA production

This study indicates that mixed culture PPB can be used to produce PHA, with sustained net yields of 21 ± 3% (on COD) (and up to 30%), and yield on accumulation only of 54 ± 2%. Peak net yields of 43% over the entire cycle, and 100% during the accumulation were achieved. The results from cycle studies indicate potential to increase sustained productivity through optimisation growth and accumulation end-points. Currently the end of cycle PHA contents averaged 35% on VS, but with a peak content in the cycle study of over 50% on VS. The peak PHA content compares well to other phototrophic and aerobic mixed, and potentially even pure culture aerobic platforms (Chen, 2009; Strong et al., 2016). The sustained volumetric productivities over the entire cycle and the accumulation were 58 ± 6 and 145 ± 14 mgPHA-COD L^{-1} d^{-1}, respectively. The cycle studies indicated that it will be important to stop accumulation prior to PHA decay, to maximise yield and PHA content. Considering detailed analysis of cycle 20 (achieving a content of 53 wt% VS) the accumulation time can be reduced to 0.7 days with a peak volumetric productivity of 0.62 gPHA-COD L^{-1} d^{-1}. These rates are comparable to peak rates achieved with mixed PPB cultures (0.48–1.3 gPHA-COD L^{-1} d^{-1} (Fradinho et al., 2019)), which are among the highest production rates reported for PPB in literature (*e.g.* compared to 0.048–2.11 gPHA-COD L^{-1} d^{-1} (Fradinho et al., 2021)). The main difference here is that the biomass can be harvested at around 100 gTS L^{-1} (up to 42 gPHA L^{-1}), compared to around 0.35–2.7 gTS L^{-1} in suspended systems in open or closed photobioreactors (Jorquera et al., 2010). The integrated up-concentration of the biomass has the potential to reduce the processing costs as (for example) centrifuges and decanters can be skipped or can be substantially downsized (note that the suspended fraction would be lost). However, scraping will also incur additional costs, particularly capital costs.

However, in comparison to aerobic PHA platforms which readily achieve 3.1–96 gPHA L^{-1} d^{-1} (Jung et al., 2001; Tamis et al., 2014), even the peak rates realised in this study are relatively low. It is noted that phototrophic PHA production is at a very early stage compared with aerobic PHA production, which has been produced from feedstocks as diverse as primary sludge, municipal waste activated sludge, crude glycerol, cheese whey, and pickle wastewater (Novelli et al., 2021), but volumetric productivity needs to be increased by an order of magnitude to be competitive with aerobic sources (even considering that higher yield on substrate can be theoretically achieved with PPB).

Some options may include a shorter, optimised cycle, focused on minimum time for accumulation and to an accumulation peak, and selection for phototrophic PHA accumulators, both of which would improve viability. PPB granulation may also assist in focusing on self-supporting biofilm option (Stegman et al., 2021). Light input is a major issue, and the economics of artificial light input mean that artificial light is unviable. The irradiance of 250 W m^{-2} applied here would result in electricity costs of $171 $kgPHA\text{-}COD^{-1}$ (assuming 3.5 gPHA-COD m^{-2} d^{-1}, 0.1 $ kWh^{-1}), which is clearly uneconomic. Even at irradiances of 6 W m^{-2} (which is low, but has been previously applied for PPB growth (Dalaei et al., 2020)), the costs for light supply only, would be >$4 kg^{-1} of PHA-COD (capex not considered), which is already higher than the value of the PHA (Pérez et al., 2020). This underlines the necessity of naturally illuminated, outdoor operation, with a possibility to accumulate during the day and grow in the night *e.g.* via a mixed metabolic mode system applying anaerobic illuminated photoheterotrophy and aerobic chemoheterotrophy at night.

3.7. Alternative utilisation routes of PHA containing PPB biomass

PHA containing PPB biomass as immuno-nutritional feed component might be an interesting alternative to actual biodegradable plastic production. This would naturally increase the volumetric productivities of PPB biomass by 58–72% (based on 53 and 35 wt% VS PHA) and save all PHA extraction related costs. PPB biomass is generally characterised by high crude protein contents, relatively favourable amino acid profiles, pigments (carotenoids and bacteriochlorophylls) and vitamins, making bulk substitution of fishmeal possible (Delamare-Debouteville et al., 2019). In addition, intracellular PHA granules might add additional functionality, potentially increasing the value of the biomass.

PHA, or more specifically short chain fatty acids (SCFA), which are by-products of microbial PHA degradation, are commercially used as antimicrobial bio-agent in commercial animal feed. While the antibacterial effects of SCFA are not clearly elucidated, a range of pathogenic enterobacteria (*Escherichia coli,* yeast, *Salmonella typhimurium, Shigella flexneri*, *Vibrio campbelli*) have been effectively inhibited in poultry (Van Immerseel et al., 2006), fish (sea bass, Nile tilapia, (Situmorang et al., 2016), and shrimps (Kiran et al., 2020). At additions of 0.5–5.0 wt% TS of PHA to the feed, the bioactive role of SCFA reduced mortalities and improved weight gains, tolerance towards stress conditions as well as disease prevention.

The average (non-optimised) PHA content of 28 wt% TS achieved in this study would require an inclusion rate of around 18 wt% TS of PPB biomass to commercial feed. PPB inclusion rates of 33% and 66% (substituting fishmeal) have been successfully tested in barramundi feed (Delamare-Debouteville et al., 2019). This means a PPB PHA content of around 15 wt% TS PHA might be sufficient to add immuno-nutritional functionality to the PPB feed product. It is highly desirable to achieve this without the limitation of nutrients in a dedicated accumulation phase as this would broaden the applicability. In this context, low amounts of PHB (2.5 wt% TS) were found in PPB grown with full nutrient supply (Delamare-Debouteville et al., 2019).

Potential advantages of the use of intracellular PHA (in the PPB cell) in feed include an increased potential to reach the gastrointestinal tract to exhibit bacteriocidal activity. This might not be achieved when liquid or powdered SCFA are applied. This is partially solved by SCFA coated feed although the applications in aquaculture are also limited due to the water-soluble character of SCFA. Another advantage might be the increased palatability of intracellular PHA and its degradation into SCFA as the foul volatile odour of SCFA is avoided. The amorphous character of intracellular PHA (in wet biomass) is also helpful as it exerts improved biotic and abiotic degradabilities (compared to crystalline PHA) in the gut of fish and crustaceans (Jendrossek and Handrick, 2002; Yu et al., 2005). This likely maximises the SCFA generation and the immuno-nutritional effects. However, there is currently no literature about intracellular PHA from PPB and the combined effects in feeds.

4. Conclusions

Mixed culture PPB accumulates relevant PHA contents of >35 wt%

VS at average yields of 21% (net growth + accumulation) or 55% (accumulation only). A shortening of the accumulation phase has the potential to increase to the PHA to >50 wt% VS while yields can be beyond 40% and >90% for net growth + accumulation and accumulation only. Up to 80% of the PHA can be harvested by biofilm removal at ~100 gTS L^{-1} (remainder in suspension). Sustained and peak volumetric productivities of 0.15 gPHA-COD L^{-1} d^{-1} and 0.62 gPHA-COD L^{-1} d^{-1} (ACC only) can be achieved. Further exploration of different cycle times and environmental conditions could help to optimise the PHA content and yield.

CRediT authorship contribution statement

Tim Hülsen: Investigation, Methodology, Writing, Writing – original draft. **Daniel Venturato:** Investigation, Methodology, Writing, Writing – original draft. **Clement Chan:** Investigation, Writing, Writing – original draft. **Luigi Vandi:** Investigation, Writing – review & editing. **Bronwyn Laycock:** Writing – review & editing, Conceptualization. **Steven Pratt:** Writing – review & editing, Conceptualization. **Samuel Stegman:** Investigation, Writing – review & editing. **Mark van Loosdrecht:** Conceptualization, Writing – review & editing. **Damien J. Batstone:** Conceptualization, Formal analysis, Writing – review & editing, Supervision.

Declaration of competing interest

We wish to confirm that there are no known conflicts of interest associated with this publication that could have influenced its outcome.

We confirm that the manuscript has been read and approved by all named authors and that there are no other persons who satisfied the criteria for authorship but are not listed. We further confirm that the order of authors listed in the manuscript has been approved by all of us.

We confirm that we have given due consideration to the protection of intellectual property associated with this work and that there are no impediments to publication, including the timing of publication, with respect to intellectual property. In so doing we confirm that we have followed the regulations of our institutions concerning intellectual property.

We further confirm that any aspect of the work covered in this manuscript that has involved either experimental animals or human patients has been conducted with the ethical approval of all relevant bodies and that such approvals are acknowledged within the manuscript.

We understand that the Corresponding Author is the sole contact for the Editorial process (including Editorial Manager and direct communications with the office). He is responsible for communicating with the other authors about progress, submissions of revisions and final approval of proofs. We confirm that we have provided a current, correct email address which is accessible by the Corresponding Author and which has been configured to accept email from d.batstone@uq.edu.au.

Data availability

Data is provided in supplementary information.

Acknowledgements

We gratefully acknowledge Nathan Clayton from the Australian Centre for Water and Environmental Biotechnology for assistance with analytical measurements. This work was funded by the Australian Government through the Australian Research Council (Project DP190102979).

Appendix A. Supplementary data

Supplementary data to this article can be found online at https://doi.org/10.1016/j.jclepro.2023.140001.

Appendices (E-supplementary data of this work can be found in online version of the paper.)

References

Alloul, A., Wuyts, S., Lebeer, S., Vlaeminck, S.E., 2019. Volatile fatty acids impacting phototrophic growth kinetics of purple bacteria: paving the way for protein production on fermented wastewater. Water Res. 152, 138–147.

Braunegg, G., Sonnleitner, B.Y., Lafferty, R.M., 1978. A rapid gas chromatographic method for the determination of poly-β-hydroxybutyric acid in microbial biomass. Eur. J. Appl. Microbiol. Biotechnol. 6, 29–37.

Capson-Tojo, G., Batstone, D.J., Grassino, M., Vlaeminck, S.E., Puyol, D., Verstraete, W., Kleerebezem, R., Oehmen, A., Ghimire, A., Pikaar, I., Lema, J.M., Hülsen, T., 2020. Purple phototrophic bacteria for resource recovery: challenges and opportunities. Biotechnol. Adv. 43, 107567.

Castro-Sowinski, S., Burdman, S., Matan, O., Okon, Y., 2010. In: Chen, G.G.-Q. (Ed.), Plastics from Bacteria: Natural Functions and Applications. Springer Berlin Heidelberg, Berlin, Heidelberg, pp. 39–61.

Chan, C.M., Johansson, P., Magnusson, P., Vandi, L.-J., Arcos-Hernandez, M., Halley, P., Laycock, B., Pratt, S., Werker, A., 2017. Mixed culture polyhydroxyalkanoate-rich biomass assessment and quality control using thermogravimetric measurement methods. Polym. Degrad. Stabil. 144, 110–120.

Chen, G.-Q., 2009. A microbial polyhydroxyalkanoates (PHA) based bio-and materials industry. Chem. Soc. Rev. 38 (8), 2434–2446.

Chen, G.Q., 2010. Industrial Production of PHA. *Plastics from Bacteria: Natural Functions and Applications*, pp. 121–132.

Cheng, M.-L., Sun, Y.-M., Chen, H., Jean, Y., 2009. Change of structure and free volume properties of semi-crystalline poly (3-hydroxybutyrate-co-3-hydroxyvalerate) during thermal treatments by positron annihilation lifetime. Polymer 50 (8), 1957–1964.

Dalaei, P., Bahreini, G., Nakhla, G., Santoro, D., Batstone, D., Hülsen, T., 2020. Municipal wastewater treatment by purple phototropic bacteria at low infrared irradiances using a photo-anaerobic membrane bioreactor. Water Res. 173, 115535.

Delamare-Deboutteville, J., Batstone, D.J., Kawasaki, M., Stegman, S., Salini, M., Tabrett, S., Smullen, R., Barnes, A.C., Hülsen, T., 2019. Mixed culture purple phototrophic bacteria is an effective fishmeal replacement in aquaculture. Water Res. X 4, 100031.

European Bioplastics and nova-Institut, 2020. Press Release: Market Update 2020. December 2. https://www.european-bioplastics.org/market-update-2020-bioplastics-continue-to-become-mainstream-as-the-global-bioplastics-market-is-set-to-grow-by-36-percent-over-the-next-5-years/. accessed on 15 July 2021.

Farghaly, A., Enitan, A.M., Kumari, S., Bux, F., Tawfik, A., 2017. Polyhydroxyalkanoates production from fermented paperboard mill wastewater using acetate-enriched bacteria. Clean Technol. Environ. Policy 19 (4), 935–947.

Feng, L., Watanabe, T., Wang, Y., Kichise, T., Fukuchi, T., Chen, G.-Q., Doi, Y., Inoue, Y., 2002. Studies on Comonomer compositional distribution of bacterial poly(3-hydroxybutyrate-co-3-hydroxyhexanoate)s and thermal characteristics of their factions. Biomacromolecules 3 (5), 1071–1077.

Fradinho, J., Allegue, L.D., Ventura, M., Melero, J.A., Reis, M.A.M., Puyol, D., 2021. Up-scale challenges on biopolymer production from waste streams by Purple Phototrophic Bacteria mixed cultures: a critical review. Bioresour. Technol. 327, 124820.

Fradinho, J.C., Oehmen, A., Reis, M.A.M., 2019. Improving polyhydroxyalkanoates production in phototrophic mixed cultures by optimizing accumulator reactor operating conditions. Int. J. Biol. Macromol. 126, 1085–1092.

Gentekos, D.T., Sifri, R.J., Fors, B.P., 2019. Controlling polymer properties through the shape of the molecular-weight distribution. Nat. Rev. Mater. 4, 761–774.

Harada, J., Mizoguchi, T., Yoshida, S., Isaji, M., Oh-oka, H., Tamiaki, H., 2008. Composition and localization of bacteriochlorophyll a intermediates in the purple photosynthetic bacterium Rhodopseudomonas sp. Rits. Photosynthesis Research 95 (2), 213–221.

Higuchi-Takeuchi, M., Morisaki, K., Toyooka, K., Numata, K., 2016. Synthesis of high-molecular-weight polyhydroxyalkanoates by marine photosynthetic purple bacteria. PLoS One 11 (8), e0160981.

Hubbell, D.H., Kidder, G., 2009. Biological Nitrogen Fixation. University of Florida IFAS Extension Publication SL16, pp. 1–4.

Hülsen, T., Batstone, D.J., Keller, J., 2014. Phototrophic bacteria for nutrient recovery from domestic wastewater. Water Res. 50 (0), 18–26.

Hülsen, T., Hsieh, K., Batstone, D.J., 2019. Saline wastewater treatment with purple phototrophic bacteria. Water Res. 160, 259–267.

Jendrossek, D., Handrick, R., 2002. Microbial degradation of polyhydroxyalkanoates. Annu. Rev. Microbiol. 56 (1), 403–432.

Jiang, Y., Marang, L., Tamis, J., van Loosdrecht, M.C., Dijkman, H., Kleerebezem, R., 2012. Waste to resource: converting paper mill wastewater to bioplastic. Water Res. 46 (17), 5517–5530.

Jorquera, O., Kiperstok, A., Sales, E.A., Embiruçu, M., Ghirardi, M.L., 2010. Comparative energy life-cycle analyses of microalgal biomass production in open ponds and photobioreactors. Bioresour. Technol. 101 (4), 1406–1413.

Jung, K., Hazenberg, W., Prieto, M., Witholt, B., 2001. Two-stage continuous process development for the production of medium-chain-length poly(3-hydroxyalkanoates). Biotechnol. Bioeng. 72 (1), 19–24.

Kai, W., He, Y., Inoue, Y., 2005. Fast crystallization of poly(3-hydroxybutyrate) and poly (3-hydroxybutyrate-co-3-hydroxyvalerate) with talc and boron nitride as nucleating agents. Polym. Int. 54 (5), 780–789.

Kiran, G.S., Priyadharshini, S., Sajayan, A., Ravindran, A., Priyadharshini, G.B., Ramesh, U., Suarez, L.E.C., Selvin, J., 2020. Dietary administration of gelatinised polyhydroxybutyrate to Penaeus vannamei improved growth performance and enhanced immune response against Vibrio parahaemolyticus. Aquaculture 517, 734773.

Kourmentza, C., Plácido, J., Venetsaneas, N., Burniol-Figols, A., Varrone, C., Gavala, H. N., Reis, M.A.M., 2017. Recent advances and challenges towards sustainable polyhydroxyalkanoate (PHA) production. Bioengineering 4 (2), 55.

Liu, L.-Y., Xie, G.-J., Xing, D.-F., Liu, B.-F., Ding, J., Ren, N.-Q., 2020. Biological conversion of methane to polyhydroxyalkanoates: current advances, challenges, and perspectives. Environmental Science and Ecotechnology 2, 100029.

Luangthongkam, P., Strong, P.J., Syed Mahamud, S.N., Evans, P., Jensen, P., Tyson, G., Laycock, B., Lant, P.A., Pratt, S., 2019. The effect of methane and odd-chain fatty acids on 3-hydroxybutyrate (3HB) and 3-hydroxyvalerate (3HV) synthesis by a Methylosinus-dominated mixed culture. Bioresources and Bioprocessing 6 (1), 50.

Luongo, V., Ghimire, A., Frunzo, L., Fabbricino, M., d'Antonio, G., Pirozzi, F., Esposito, G., 2017. Photofermentative production of hydrogen and poly-β-hydroxybutyrate from dark fermentation products. Bioresour Technol 228, 171–175. https://doi.org/10.1016/j.biortech.2016.12.079. Epub 2016 Dec 24. PMID: 28063359.

Manz, W., Amann, R., Ludwig, W., Wagner, M., Schleifer, K.-H., 1992. Phylogenetic oligodeoxynucleotide probes for the major subclasses of proteobacteria: problems and solutions. Syst. Appl. Microbiol. 15 (4), 593–600.

Martínez-Reyes, I., Chandel, N.S., 2020. Mitochondrial TCA cycle metabolites control physiology and disease. Nat. Commun. 11 (1), 102.

Melnicki, M.R., Eroglu, E., Melis, A., 2009. Changes in hydrogen production and polymer accumulation upon sulfur-deprivation in purple photosynthetic bacteria. Int. J. Hydrogen Energy 34 (15), 6157–6170.

Montiel-Corona, V., Buitrón, G., 2021. Polyhydroxyalkanoates from organic waste streams using purple non-sulfur bacteria. Bioresour. Technol. 323, 124610.

Novelli, L.D.D., Sayavedra, S.M., Rene, E.R., 2021. Polyhydroxyalkanoate (PHA) production via resource recovery from industrial waste streams: a review of techniques and perspectives. Bioresour. Technol. 331, 124985.

Obruca, S., Sedlacek, P., Koller, M., 2021. The underexplored role of diverse stress factors in microbial biopolymer synthesis. Bioresour. Technol. 326, 124767.

Oehmen, A., Keller-Lehmann, B., Zeng, R.J., Yuan, Z., Keller, J., 2005. Optimisation of poly-β-hydroxyalkanoate analysis using gas chromatography for enhanced biological phosphorus removal systems. J. Chromatogr. A 1070 (1), 131–136.

Pearce, R.P., Marchessault, R.H., 1994. Melting and crystallization in bacterial poly (β-hydroxyvalerate), PHV, and blends with poly(β-hydroxybutyrate-co-hydroxyvalerate). Macromolecules 27 (14), 3869–3874.

Pérez, V., Mota, C.R., Muñoz, R., Lebrero, R., 2020. Polyhydroxyalkanoates (PHA) production from biogas in waste treatment facilities: assessing the potential impacts on economy, environment and society. Chemosphere 255, 126929.

Reis, M.A., Serafim, L.S., Lemos, P.C., Ramos, A.M., Aguiar, F.R., Van Loosdrecht, M.C., 2003. Production of polyhydroxyalkanoates by mixed microbial cultures. Bioproc. Biosyst. Eng. 25 (6), 377–385.

Revelles, O., Tarazona, N., García, J.L., Prieto, M.A., 2016. Carbon roadmap from syngas to polyhydroxyalkanoates in Rhodospirillum rubrum. Environ. Microbiol. 18 (2), 708–720.

Salehizadeh, H., Van Loosdrecht, M.C., 2004. Production of polyhydroxyalkanoates by mixed culture: recent trends and biotechnological importance. Biotechnol. Adv. 22 (3), 261–279.

Sali, S., Mackey, H.R., 2021. The application of purple non-sulfur bacteria for microbial mixed culture polyhydroxyalkanoates production. Rev. Environ. Sci. Biotechnol. 20, 959–983.

Situmorang, M.L., De Schryver, P., Dierckens, K., Bossier, P., 2016. Effect of poly-β-hydroxybutyrate on growth and disease resistance of Nile tilapia Oreochromis niloticus juveniles. Vet. Microbiol. 182, 44–49.

Stegman, S., Batstone, D.J., Rozendal, R., Jensen, P.D., Hülsen, T., 2021. Purple phototrophic bacteria granules under high and low upflow velocities. Water Res. 190, 116760.

Strong, P., Laycock, B., Mahamud, S., Jensen, P., Lant, P., Tyson, G., Pratt, S., 2016. The opportunity for high-performance biomaterials from methane. Microorganisms 4 (1), 11.

Tamis, J., Lužkov, K., Jiang, Y., Loosdrecht, M.C.M.v., Kleerebezem, R., 2014. Enrichment of Plasticicumulans acidivorans at pilot-scale for PHA production on industrial wastewater. J. Biotechnol. 192, 161–169.

Van Immerseel, F., Russell, J.B., Flythe, M.D., Gantois, I., Timbermont, L., Pasmans, F., Haesebrouck, F., Ducatelle, R., 2006. The use of organic acids to combat Salmonella in poultry: a mechanistic explanation of the efficacy. Avian Pathol. 35 (3), 182–188.

Werker, A.G., Jannasch, P., Johansson, P.S.T., Magnusson, P.O.G., Maurer, F.H.J., 2010. Method for Recovery of Stabilized Polyhydroxyalkanoates from Biomass that Has Been Used to Treat Organic Waste Patent: US9487624B2.

Werker, A.G., Johansson, P.S.T., Magnusson, P.O.G., 2014. Process for the Extraction of Polyhydroxyalkanoates from Biomass Patent: US20150368393A1.

Yu, J., Plackett, D., Chen, L.X.L., 2005. Kinetics and mechanism of the monomeric products from abiotic hydrolysis of poly[(R)-3-hydroxybutyrate] under acidic and alkaline conditions. Polym. Degrad. Stabil. 89 (2), 289–299.